

# Effects of growth temperature on high-quality $\text{In}_{0.2}\text{Ga}_{0.8}\text{N}$ layers by plasma-assisted molecular beam epitaxy\*

Zhang Dongyan(张东炎)<sup>1,2</sup>, Zheng Xinhe(郑新和)<sup>1,†</sup>, Li Xuefei(李雪飞)<sup>1</sup>,  
Wu Yuanyuan(吴渊渊)<sup>1,2</sup>, Wang Jianfeng(王建峰)<sup>1</sup>, and Yang Hui(杨辉)<sup>1</sup>

<sup>1</sup>Key Laboratory of Nanodevices and Applications, Suzhou Institute of Nano-Tech and Nano-Bionics, Chinese Academy of Sciences, Suzhou 215125, China

<sup>2</sup>Graduate University of the Chinese Academy of Sciences, Beijing 100049, China

**Abstract:** High-quality  $\text{In}_{0.2}\text{Ga}_{0.8}\text{N}$  epilayers were grown on a GaN template at temperatures of 520 and 580 °C via plasma-assisted molecular beam epitaxy. The X-ray rocking curve full widths at half maximum (FWHM) of (10.2) reflections is 936 arcsec for the 50-nm-thick InGaN layers at the lower temperature. When the growth temperature increases to 580 °C, the FWHM of (00.2) reflections for these samples is very narrow and keeps similar, while significant improvement of (10.2) reflections with an FWHM value of 612 arcsec has been observed. This improved quality in InGaN layers grown at 580 °C is also reflected by the much larger size of the crystalline column from the AFM results, stronger emission intensity as well as a decreased FWHM of room temperature PL from 136 to 93.9 meV.

**Key words:** InGaN; PA-MBE; quality; solar cells

**DOI:** 10.1088/1674-4926/33/10/103001

**EEACC:** 2520D

## 1. Introduction

Currently, high performance photovoltaic devices are exclusively based on a GaInP/(In)GaAs/InGaAs tandem solar cell with an efficiency higher than 42.1%<sup>[1]</sup>. In order to achieve higher photovoltaic efficiencies, a sub-cell with a band gap greater than 2.66 eV is required<sup>[2]</sup>. Such a high band-gap is not readily available in other established material systems. Acting as a sub-cell,  $\text{In}_x\text{Ga}_{1-x}\text{N}$  solar cells with an effective absorption and photo-current generation in the spectral range of 365–460 nm can significantly enhance the conversion efficiency of light in this spectral range. But, it is still difficult to grow high quality  $\text{In}_x\text{Ga}_{1-x}\text{N}$  layers with In-mole fractions in the range of  $x \geq 0.2$  due to the lack of lattice-matched substrates, high lattice mismatch and the significant difference of optimal growth conditions between the alloy components of GaN and InN<sup>[3–5]</sup>. The high density of crystalline defects deteriorates the device performance and still is a major technological challenge for applications<sup>[6]</sup>.

InGaN bulk layers have been grown by a variety of techniques including molecular beam epitaxy (MBE) and metal-organic vapour phase epitaxy (MOVPE). To improve the crystalline quality, growth parameters like the temperature, III/V ratio, etc. are optimized<sup>[7–11]</sup>. Very recently, Kraus *et al.* reported that under metal-rich conditions by PA-MBE, the FWHM of 51-nm-thick InGaN layers with a content of 18.6% was 160 meV for PL results<sup>[12]</sup>. Gorge *et al.* reported a MOVPE growth of 140-nm-thick InGaN layers with an In composition of 19.5% showing an XRC FWHM of approximately 610 arcsec for (00.2) reflections<sup>[13]</sup>. Moseley *et al.*

reported that the 51-nm-thick InGaN layers grown by metal-modulated epitaxy, with a content of 22%, had an XRC FWHM of 362 arcsec for (00.2) reflections<sup>[14]</sup>. However, to the best of our knowledge, there were few reports about XRC FWHM of asymmetrical reflections like (10.2) or (10.5) for InGaN layers<sup>[15, 16]</sup>. The improvement of crystalline quality of InGaN layers is still an essential requirement for the preparation of 2.66 eV-top cells.

In this paper, MBE-grown  $\text{In}_{0.2}\text{Ga}_{0.8}\text{N}$  layers which have comparable crystalline quality to those obtained by Huang using MOVPE<sup>[16]</sup> were demonstrated. Also, we intentionally kept the In composition constant, and optimization of III/V supply ratio clarified the effect of growth temperature on crystalline quality by MBE. We used a KSA BandiT to monitor changes in temperature during growth. The BandiT system measured the temperature-dependent bandgap of a GaN template in order to provide an accurate method to control temperature. The temperature dependence of InGaN layers were investigated in terms of structure, surface and photoluminescence (PL) measurements.

## 2. Experimental

Samples used in this study were grown by PA-MBE in a Veeco Gen 20A system equipped with standard effusion cells for Ga and In. (00.1)-GaN templates, grown by MOVPE, with a threading dislocation density in the  $(3\sim 10) \times 10^8 \text{ cm}^{-3}$  range were used as substrates. The templates with a thickness of around 3.8  $\mu\text{m}$  were grown on a *c*-plane sapphire. After a chemical degrease, the substrates were introduced to the MBE system and outgassed at 200 °C for 30 min, followed by a ther-

\* Project supported by the SONY-SINANO Joint Project (No. Y1AAQ11001), the Suzhou Solar Cell Research Project (No. ZXJ0903), and the Ministry of Science and Technology of China (No. 2010DFA22770).

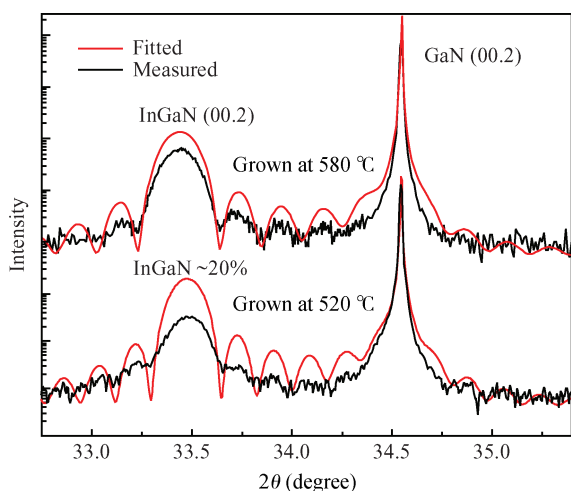
† Corresponding author. Email: xhzheng2009@sinano.ac.cn

Received 4 March 2012, revised manuscript received 11 April 2012

© 2012 Chinese Institute of Electronics

Table 1. Comparison of quality and crystalline grain size measured by XRD, PL and AFM.

Sample	XRC FWHM (arcsec)		FWHM of PL (meV)	Crystalline grain size (nm)
	(00.2)	(10.2)		
Grown at 520 °C	496	936	136	~ 70
Grown at 580 °C	468	612	93.9	~ 800

Fig. 1. Measured and fitted XRD  $\omega$ - $2\theta$  curves in the vicinity of (00.2) reflections for InGaN/GaN layers grown at various temperatures.

mal clean process at 600 °C for 1 h. Prior to InGaN growth, a 50-nm-thick GaN layer was grown at 650 °C under intermediate Ga-rich conditions to obtain a smooth and reproducible surface. Active nitrogen was supplied using a UNI-bulb radio frequency (RF) plasma N source with a RF power of 330 W. The nitrogen flux was kept constant at 1.5 sccm at a growth chamber pressure of  $1.32 \times 10^{-5}$  Torr. The growth of InGaN layers at 520 and 580 °C was monitored by in-situ reflection high-energy electron diffraction (RHEED).

X-ray diffraction (XRD) was performed using a D8/Bruker DISCOVER high-resolution X-ray diffractometer, equipped with a four-crystal monochromator in Ge (220) and Ge (440) configuration and four-circle translational capability. The photoluminescence (PL) was excited by a 325 nm line of a He-Cd laser with an excitation power of 20 mW. Investigations of the surface morphologies were carried out by optical microscopy and atomic force microscopy (AFM). For as-grown samples, no metal droplets were observed on the surfaces.

### 3. Results and discussion

Coherent  $\omega$ - $2\theta$  diffraction curves measured in the vicinity of (00.2) reflections for InGaN layers grown at 520 °C and 580 °C in Fig. 1 have strong diffraction peaks. Both samples exhibit an In content of approximately 20% from the fitted curves in combination with degrees of relaxations measured by reciprocal space mappings (RSM) later<sup>[17]</sup>. Clear interface fringes around the InGaN peak indicate the perfect interface between the InGaN and GaN layer without an appearance of a transformation sublayer or secondary dislocation loops in the volume of InGaN layers<sup>[6, 18]</sup>, from which thickness of about 51 and 45 nm are determined for InGaN layers grown at 520 and 580 °C, respectively. The calculated thickness corresponds

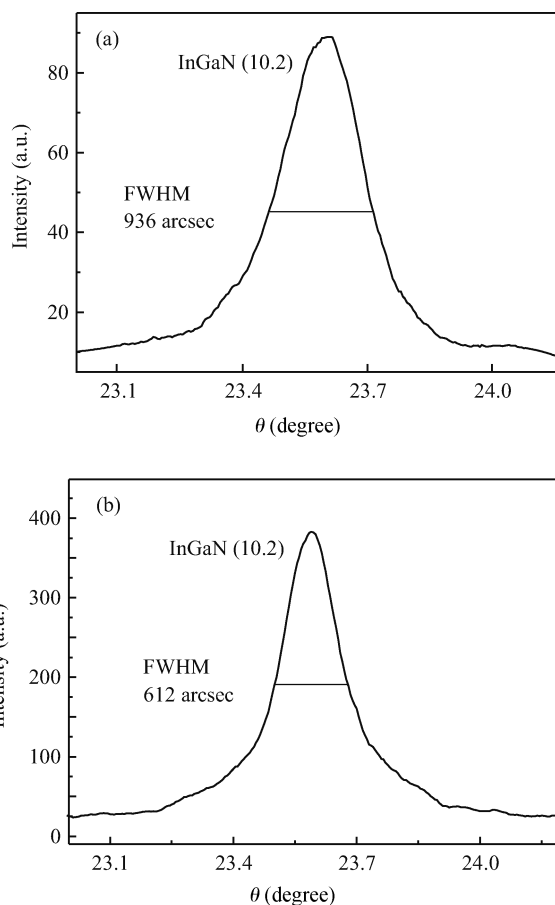


Fig. 2. XRC of asymmetrical (10.2) reflections for InGaN layers grown at (a) 520 and (b) 580 °C.

well with the expected value in term of the growth rate.

To better analyze temperature dependence on the crystalline quality of III nitrides, the FWHM of XRCs from symmetrical and asymmetrical reflections is frequently used as figure of merit<sup>[19]</sup>. Figure 2 shows XRCs of asymmetrical reflections for InGaN layers grown at 520 and 580 °C. The FWHM of (10.2) for InGaN layers grown at 520 °C is 936 arcsec. While the growth temperature increases to 580 °C, improvement in the quality of InGaN layers reflected by a narrower FWHM of 612 arcsec has been observed, shown in Table 1. Note that the FWHM of the (00.2) reflections for these samples grown at different temperatures remains similar. Better crystalline quality for the higher growth temperature is comparable to the value reported in Ref. [16]. Since XRC FWHMs of asymmetrical and symmetrical reflections involve the density of edge or mixed and of screw dislocations in the InGaN layers<sup>[20]</sup>, the density of edge or mixed dislocations in InGaN layers grown at high temperatures is much lower than that grown at 520 °C. In the epitaxy growth of III nitrides, edge or mixed dislocations will generate among column grain boundary during island or subgrain

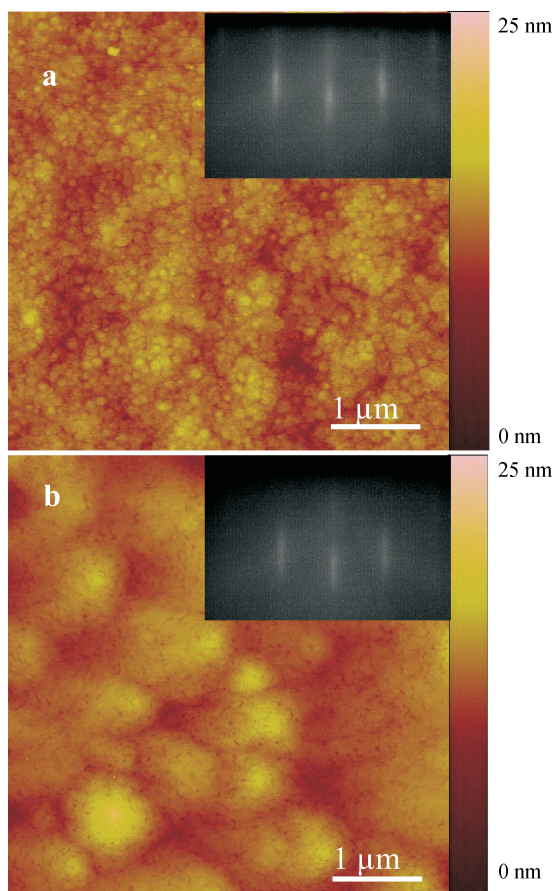


Fig. 3. AFM images ( $5 \times 5 \mu\text{m}$ ) of InGaN layers grown at (a) 520 and (b) 580 °C under metal-rich growth conditions. Inset: the corresponding RHEED patterns during growth.

coalescence<sup>[20, 21]</sup>. At high temperatures, due to the enhanced diffusivity of the metal adatom on the surface, subgrains of a larger size will easily form. The average size is characterized by AFM images, shown in Fig. 3.

Judging from Fig. 3, we can see that the InGaN samples show the larger size of columnar grains in the conditions of higher temperature as compared with lower temperature. The average grain size of the InGaN layers grown at higher temperature is estimated to be 800 nm from the AFM results by line scan, which is far larger than that grown at a lower temperature. Due to the larger size of columnar grains, the lesser grain boundary will come into being when they coalesce. Therefore, the lower density of edge or mixed is generated for the resulting epilayers. Additionally, it is interesting to note that two samples show a similar RMS roughness, that is 1.41 and 1.58 nm for the InGaN layers grown at 520 and 580 °C, respectively. The results could be ascribed to well-controlled metal-rich conditions at a reasonable Ga/In supply ratio with a 2D growth for both samples identified from the RHEED patterns in the insets of Fig. 3.

Interestingly, the higher quality as-grown InGaN layers were further reflected by PL measurements. Figure 4 shows the room temperature PL spectra of the InGaN layers grown at 520 and 580 °C with the peak energy of InGaN epilayers corresponding well to an In content of 20% estimated from XRD results. It is worth noting that the PL intensity of the InGaN

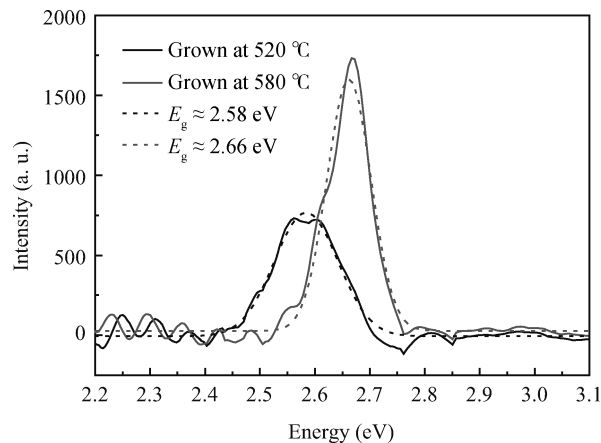


Fig. 4. Room temperature PL spectra (solid line) of InGaN layers grown at lower and higher temperatures and fitted curves by the Gaussian numerical function (short dashed line).

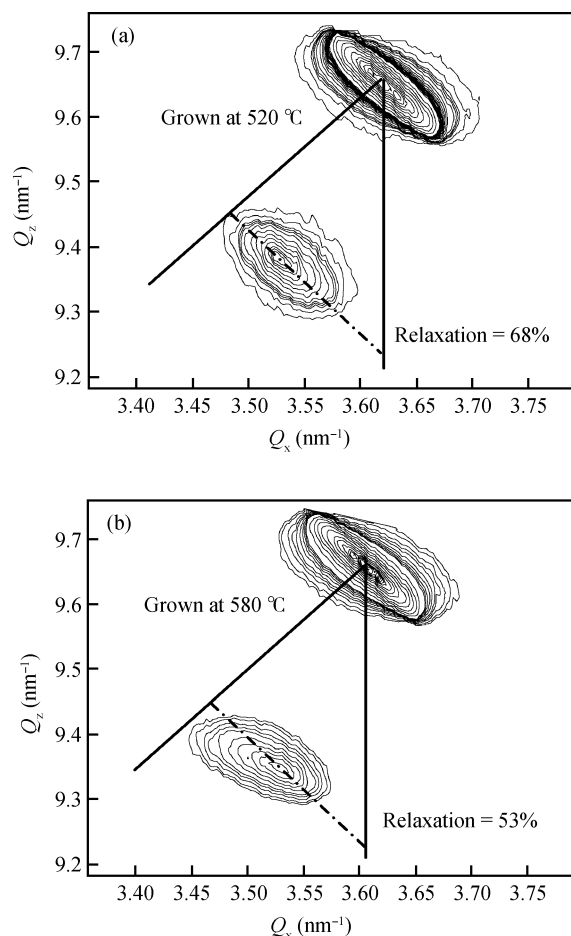


Fig. 5. RSM of asymmetric (10.5) reflections for the two InGaN/GaN samples.

layers grown at higher temperature is 2.5 times stronger than that grown at 520 °C. This enhancement in PL intensity could be attributed to a reduction of mixed or edge-type dislocation density that is regarded as an origin of non-radiative recombination centers<sup>[22–24]</sup>. The additional peaks and shoulders besides the main peak are corresponding to Fabry Perot interference between the GaN/sapphire interface and the surface. The

fitted curves for the PL spectra by the Gaussian numerical function, also shown in Fig. 4 (short dashed line), are used to accurately determine the peak positions and FWHM. Compared to InGaN layers grown at 580 °C, a longer wavelength of PL peak position for the InGaN layers grown at 520 °C was observed. Actually, strain relaxation in InGaN bulk layers can lead to a red-shift of peak emission for PL measurements<sup>[3]</sup>. So the red-shift in the InGaN layers grown at 520 °C may contribute to the larger degree of relaxation (68%) as compared with that of the relaxation (53%) in the InGaN layers at 580 °C, determined by RSM shown in Fig. 5. Actually, the difference in the relaxation degree of these as-grown samples is also reflected by a small change in their thickness. The samples grown at 520 °C are slightly thicker (51 nm) which could lead to more relaxation compared to those grown at 580 °C (45 nm). Using the curve fitting analysis, the higher-temperature samples show a FWHM 93.9 meV, which is narrower than that of the lower temperature sample (136 meV). The improvement in the structural and optical properties of In<sub>0.2</sub>Ga<sub>0.8</sub>N epilayers at higher growth temperatures indicates a potential to realize 2.66 eV-top InGaN solar cells.

#### 4. Conclusions

High quality In<sub>0.2</sub>Ga<sub>0.8</sub>N layers with an XRC FWHM of 612 arcsec for (10.2) reflections were obtained at a high-growth temperature of 580 °C. Meanwhile, the as-grown samples show a better optical quality that is reflected by a stronger recombination intensity and narrower width of PL measurements as compared with the InGaN layers grown at 520 °C. The results could imply that a higher growth temperature and reasonable Ga/In supply ratio may be critical to obtain a high quality and low density of non-radiative recombination centers in InGaN layers which is required in high-efficiency top sub-cells.

#### References

- [1] Yamaguchi M, Takamoto T, Araki K, et al. Present and future of high efficiency multi-junction solar cells. *Lasers and Electro-Optics (CLEO)*, 2011, CMT5(1)
- [2] Barnett A, Kirkpatrick D, Honsberg C, et al. Milestones toward 50% efficient solar cell modules. *The 22nd European Photovoltaic Solar Energy Conference*, 2007
- [3] Wu J Q. When group-III nitrides go infrared: new properties and perspectives. *J Appl Phys*, 2009, 106(1): 011101
- [4] Bhuiyan A G, Hashimoto A, Yamamoto A. Indium nitride (InN): a review on growth, characterization, and properties. *J Appl Phys*, 2003, 94(5): 2779
- [5] Nanishi Y, Saito Y, Yamaguchi T. RF-molecular beam epitaxy growth and properties of InN and related alloys. *Jpn J Appl Phys I*, 2003, 42(5A): 2549
- [6] Faleev N, Honsberg C, Jani O, et al. Crystalline perfection of GaN and AlN epitaxial layers and the main features of structural transformation of crystalline defects. *J Cryst Growth*, 2007, 300(1): 246
- [7] Huang Y, Jani O, Park E H, et al. Influence of growth conditions on phase separation of InGaN bulk material growth by MOCVD. *Proceedings of the Material Research Society Symposium*, 2007, 955(107): 20
- [8] Iliopoulos E, Georgakilas A, Dimakis E, et al. InGaN (0001) alloys grown in the entire composition range by plasma assisted molecular beam epitaxy. *Phys Status Solidi A*, 2006, 203(1): 102
- [9] Nath D N, Gur E, Ringel S A, et al. Growth model for plasma-assisted molecular beam epitaxy of N-polar and Ga-polar In<sub>(x)</sub>Ga<sub>(1-x)</sub>N. *J Vac Sci Technol B*, 2011, 29(2): 021206
- [10] Das A, Magalhaes S, Kotsar Y, et al. Indium kinetics during the plasma-assisted molecular beam epitaxy of semipolar (11 $\bar{2}$ ) InGaN layers. *Appl Phys Lett*, 2010, 96(18): 181907
- [11] Komaki H, Katayama R, Onabe K, et al. Nitrogen supply rate dependence of InGaN growth properties, by RF-MBE. *J Cryst Growth*, 2007, 305(1): 12
- [12] Kraus A, Hammadi S, Hisek J, et al. Growth and characterization of InGaN by RF-MBE. *J Cryst Growth*, 2011, 323(1): 72
- [13] Gorge V, Djebbour Z, Migan-Dubois A, et al. Link between crystal quality and electrical properties of metalorganic vapour phase epitaxy In<sub>(x)</sub>Ga<sub>(1-x)</sub>N thin films. *Appl Phys Lett*, 2011, 99(6): 062113
- [14] Moseley M, Lowder J, Billingsley D, et al. Control of surface adatom kinetics for the growth of high-indium content InGaN throughout the miscibility gap. *Appl Phys Lett*, 2010, 97(19): 191902
- [15] Kim D J, Moon Y T, Song K M, et al. Effect of growth pressure on indium incorporation during the growth of InGaN by MOCVD. *J Electron Mater*, 2001, 30(2): 99
- [16] Huang Y, Melton A, Jampana B, et al. Compositional instability in strained InGaN epitaxial layers induced by kinetic effects. *J Appl Phys*, 2011, 110(6): 064908
- [17] Linyu S, Jincheng Z, Hao W, et al. Growth of InGaN and double heterojunction structure with InGaN back barrier. *Journal of Semiconductors*, 2010, 31(12): 123001
- [18] Faleev N, Jampana B, Jani O, et al. Correlation of crystalline defects with photoluminescence of InGaN layers. *Appl Phys Lett*, 2009, 95(5): 051915
- [19] Moram M A, Vickers M E. X-ray diffraction of III-nitrides. *Reports on Progress in Physics*, 2009, 72(3): 036502
- [20] Zheng X H, Chen H, Yan Z B, et al. Determination of twist angle of in-plane mosaic spread of GaN films by high-resolution X-ray diffraction. *J Cryst Growth*, 2003, 255(1-2): 63
- [21] Heying B, Wu X H, Keller S, et al. Role of threading dislocation structure on the X-ray diffraction peak widths in epitaxial GaN films. *Appl Phys Lett*, 1996, 68(5): 643
- [22] Kaneta A, Funato M, Narukawa Y, et al. Direct correlation between nonradiative recombination centers and threading dislocations in InGaN quantum wells by near-field photoluminescence spectroscopy. *Phys Status Solidi C*, 2006, 3(6): 1897
- [23] Cremades A, Piqueras J. Study of carrier recombination at structural defects in InGaN films. *Mater Sci Eng B-Solid*, 2002, 91/92: 341
- [24] Lockrey M N, Phillips M R. Characterisation of the optical properties of InGaN MQW structures using a combined SEM and CL spectral mapping system. *Journal of Semiconductors*, 2011, 32(1): 012001